

Transient fluorescence in synchronously dividing *Escherichia coli*

(balanced growth/flavin/light scattering/nonlinear model/Raman spectroscopy)

SCOTT P. LAYNE*, IRVING J. BIGIO†, ALWYN C. SCOTT*‡, AND PETER S. LOMDAHL*

*Center for Nonlinear Studies and †Chemistry Division, Los Alamos National Laboratory, Los Alamos, NM 87545

Communicated by John Wheatley, July 11, 1985

ABSTRACT Using a spectrometer equipped with an optical multichannel analyzer as the detector, we observed the Stokes laser-Raman spectra of metabolically synchronous *Escherichia coli* from 100 to 2100 cm^{-1} . After more than 400 separate recordings, at cell concentrations of 10^7 – 10^8 per ml, no Raman lines attributable to the metabolic process nor to the cells themselves were found. However, we did find that synchronous *E. coli* cultures become more fluorescent during a limited phase of the division cycle. This transient increase in fluorescence may be ascribed to a variation in the redox state of a chemical species within the bacteria or to a variation of the intracellular optical field. The effect is reproducible in synchronous cultures and it is not seen in asynchronous ones. The results suggest that spectral features seen in previous laser-Raman spectra of synchronous bacteria (taken with scanning monochromators) are due to a time-dependent variation in bacterial fluorescence.

Over the past two decades considerable interest has focused on the possibility that biological macromolecules support collective excitations. Such excitations are supposed to extend over large regions of a protein or DNA macromolecule and are expected to have unusually long lifetimes because of nonlinear interactions. The first biophysical theory to point this out was developed by Fröhlich (1, 2). In this generic theory, a collection of oscillators interact nonlinearly as they exchange quanta with an ambient heat bath. When metabolic energy pumps these oscillators, a coherent state evolves that is reminiscent of a Bose-Einstein condensation. Later, Davydov (3, 4) proposed a complementary but more specific model for energy transport in α -helical proteins. In this theory, ATP hydrolysis transfers energy to amide-I vibrations (mainly C=O stretch) in the peptide groups of a helix. Dissipation due to dipole-dipole coupling among amide-I groups is overcome by nonlinear interactions involving hydrogen bonds. The balance between dispersion and nonlinearity results in a solitary wave (soliton) that travels along the helix. Like Fröhlich's condensation, the Davydov soliton encompasses an ensemble of individual oscillators. Additional theoretical studies by Bilz *et al.* (5), Cooper (6), and Del Giudice *et al.* (7) have emphasized that extended nonlinear excitations may be a basic property of biological systems. Such ideas suggest that macromolecules in living organisms may exhibit collective vibrations in the range of 10^{11} to 10^{14} Hz. Therefore, both microwave and Raman spectroscopy should be useful tools in the search for collective states in the molecules of living organisms.

In 1968 and 1969, Webb and coworkers (8, 9) made the discovery that microwave radiation alters bacterial growth at unexpectedly narrow and specific frequencies. This surprising result has been confirmed several times (10, 11), most recently by the experiments of Grundler and Keilmann (12). Subsequently, Webb (13) reported that cultures of *Bacillus*

megaterium and *Escherichia coli* displayed complex Raman spectra from 50 to 2600 cm^{-1} when they were metabolically active. These Raman bands were not seen in dormant cultures of bacteria and division synchrony increased the likelihood of observation. This evidence suggested that collective and nonlinear excitations had been observed in living organisms.

In 1981, Scott (14) suggested the assignment of Webb's low-frequency Raman data to internal soliton vibrations, and subsequent detailed numerical analysis by Lomdahl *et al.* (15) support this assignment. Thus it appeared that Davydov's idea had found experimental support. However, reports appeared from Cooper and Amer (16), Furia and Gandhi (17), and Kinoshita *et al.* (18) that failed to confirm Webb's findings. On the other hand, reports by Drissler and Macfarlane (19), Bannikov *et al.* (20), and Drissler and Santo (21) confirmed Webb's observations. Since we are interested in a possible relationship between Davydov's theory and Webb's experiments (22–26), we decided to repeat the laser-Raman experiments using *E. coli*.

To date, all the reported laser-Raman studies of metabolically active bacteria have been performed with scanning monochromators. O'Sullivan and Santo (27) have pointed out that serious artifacts may result from such instruments. Most importantly, for scanning spectrometers they showed that variations in both the flow (or motion) of bacteria as they are presented to the laser beam and in bacterial fluorescence with time may cause the baseline of the spectrum to vary. This baseline variation can result in the appearance of false Raman peaks, as the wavelength setting of a monochromator is scanned in time. To avoid these problems, we used a polychromator equipped with an optical multichannel analyzer (OMA). Such a system is immune to false Raman peaks, due to baseline instability, because it examines a broad spectral range at one time and does not scan. In addition, we use a reliable method of bacterial synchronization in conjunction with a highly studied strain of *E. coli* that does not form clumps.

MATERIALS AND METHODS

Each experimental run consisted of three basic procedures. For all experiments, these procedures were completed on the same day (except for the growth of asynchronous parental cultures).

Growth and Synchronization of Bacteria. General guidelines for preparing minimally perturbed synchronous cultures of bacteria have been reviewed by Helmstetter (28) and Lloyd *et al.* (29). These guidelines effect a state of steady growth termed "balanced": a state in which every component of the cell culture increases by the same factor per unit time. For our experiments, we use the procedures developed

The publication costs of this article were defrayed in part by page charge payment. This article must therefore be hereby marked "advertisement" in accordance with 18 U.S.C. §1734 solely to indicate this fact.

Abbreviation: OMA, optical multichannel analyzer.

‡Present address: Department of Electrical and Computer Engineering, University of Arizona, Tucson, AZ 85721

by Helmstetter (28, 30) to synchronize *E. coli* B/r (ATCC 12407, obtained from Helmstetter).

Minimal medium contained 2 g of NH_4Cl , 6 g of Na_2HPO_4 , 3 g of KH_2PO_4 , 3 g of NaCl , 0.25 g of MgSO_4 , and 1 g of glucose per liter of purified water. All bacterial growth, synchronization, and measurement (except Coulter counting) were conducted at $37.5^\circ\text{C} \pm 0.5^\circ\text{C}$. To start, 150 ml of minimal medium was inoculated at 10^3 – 10^6 organisms per ml and allowed to grow overnight in a gyro-motion water bath. When this asynchronous culture reached 1 – 2×10^8 organisms per ml (12–20 hr), it was transferred by suction to a 142-mm-diameter filter paper (Millipore GSWP 142) while housed at constant temperature (Precision Scientific full view incubator). Next the filter and its holder were inverted and gently eluted with fresh minimal medium at 1–2 ml per min by gravity flow. After washing the filter for 20–30 min, bacteria were collected from the effluent at 5 min intervals (total volume, 5–10 ml) for Raman spectroscopy. The effluent contained daughter bacteria that divided synchronously. Typical starting concentrations of synchronous bacteria ranged from 1 to 5×10^7 per ml and, at these concentrations, the solutions were visually clear to slightly turbid. Doubling times for our synchronous *E. coli* ranged from 44 to 54 min.

Laser-Raman Spectroscopy. The spectrometer/detector system consisted of a Spex Triplemate polychromator in conjunction with an OMA. For this OMA system (EG&G/P.A.R. OMA-2) the detector was an intensified Reticon (silicon photodiode) array (P.A.R. model 1420) with ≈ 800 active elements over a 2-cm length. With this detector at the exit plane of the spectrometer and with a 1200-groove per mm holographic grating, the recorded free spectral range was $\approx 800 \text{ cm}^{-1}$ (for a center wavelength set at $\approx 550 \text{ nm}$). Typical spectral resolution was $\approx 3 \text{ cm}^{-1}$. The OMA was interfaced to transmit data files to a larger mainframe computer for subsequent analysis. Laser illumination was provided by an argon-ion laser, tuned to the 514.5-nm line, with power settings from 300 to 500 mW.

Samples of synchronous or asynchronous bacteria were placed in the temperature-controlled holding vessel shown in Fig. 1A. Then, the laser beam was multipassed through the optical cuvette while a steady flow of bacteria was maintained by gravity draw. Bacteria were exposed only once to the laser beam and, with the flow rates used (0.10–0.15 ml/min), the maximum time that any cell spent in the illuminating volume was 1–2 sec. Raman scattered light at both 90° and 270° was collected with $f/1$ optics and imaged onto the spectrometer entrance slit at $f/6$ (to match the f -number of the spectrometer) as shown in Fig. 1B. Integration times for recorded spectra ranged from 30 to 300 sec, with the 800-cm^{-1} band-pass variously adjusted to cover the

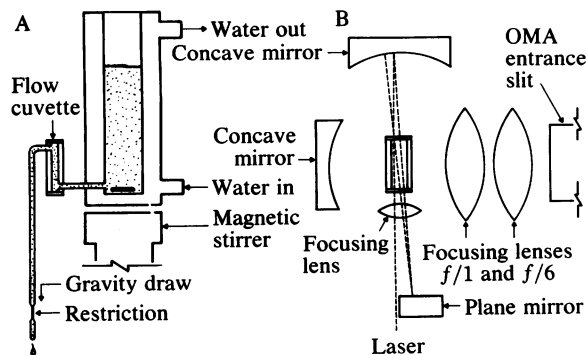


FIG. 1. (A) Bacteria in the temperature-controlled holding vessel were gently stirred with a small magnetic bar. (B) The laser beam was multipassed through the optical cuvette. This drawing shows three laser passes but typically the number was five to seven.

range from 100 to 2100 cm^{-1} on the Stokes side of the laser line.

Coulter Counting. All cultures of bacteria that were measured by Raman spectroscopy were particle counted. This demonstrated the viability of the cultures and allowed for correlations between spectra and bacterial activity. For all work, a Coulter Counter (model ZB) with a $30\text{-}\mu\text{m}$ orifice was used; it was isolated in a Faraday cage to minimize interference. Following the recommendations of Kubitschek (31) and Koch (32), samples for counting were fixed in a 0.9% NaCl (wt/vol)/0.4% formaldehyde (vol/vol) solution that had been previously passed through a $0.2\text{-}\mu\text{m}$ filter. Total counts were kept between 5000 and 25,000 bacteria, by dilution with fixer, to minimize coincidence. Each sample was counted three times and the counts were averaged. Background counts were subtracted from averaged counts to obtain final bacterial concentrations. Typical backgrounds ranged from 1 to 5% of total counts.

RESULTS

Our spectroscopic study of active *E. coli* cultures required 6 months to complete and progressed as two separate phases (Table 1). For the first phase, Raman spectra were taken over three frequency bands (100 – 830 , 530 – 1320 , and 1200 – 2100 cm^{-1}) with longer integration times ranging from 2 to 5 min. With synchronous cultures spectra were recorded before the fission cycle, during the fission cycle, and after the fission cycle, but no Raman bands were observed that could be assigned to the bacteria or to the metabolic process. However, in many spectra changes were seen in a background fluorescence that peaked around 1300 cm^{-1} (red shifted from the laser line). With asynchronous cultures we recorded spectra at concentrations ranging from 1×10^7 to 1×10^8 cells per ml and again, no Raman features appeared.

For the second phase, Raman measurements were restricted to the region from 960 to 1730 cm^{-1} and were limited to the shorter integration time of 30 sec. This region was selected because it contained Raman bands of both minimal medium and water that acted as intensity standards and also because previous publications emphasized it as an active area for Raman spectroscopy (13, 21). The shorter integration time was chosen to record many sequential Raman spectra and to preclude the possibility that, with longer integration times, short-lived spectroscopic events would be lost in the background noise. All spectra discussed below come from the second phase of work.

A typical time sequence of Raman spectra of minimal medium is shown in Fig. 2. These spectra were recorded over an interval of 10 min, with 30-sec integrations for each spectrum, or track, and 30 sec between tracks. Similar data-collection rates were used for all subsequent recordings with bacteria. Bands occurring at 980 cm^{-1} are assigned to Na_2HPO_4 and MgSO_4 , those at 1070 cm^{-1} to KH_2PO_4 , and

Table 1. Summary of measurements

Raman shift, cm^{-1}	Culture type	Cultures, no.	Spectra, no.
First-phase experiments			
100–830	Synchronous	6	25
	Asynchronous	2	8
530–1320	Synchronous	3	11
	Asynchronous	2	4
1200–2100	Synchronous	3	12
	Asynchronous	2	2
Second-phase experiments			
960–1730	Synchronous	7	246
	Asynchronous	3	155

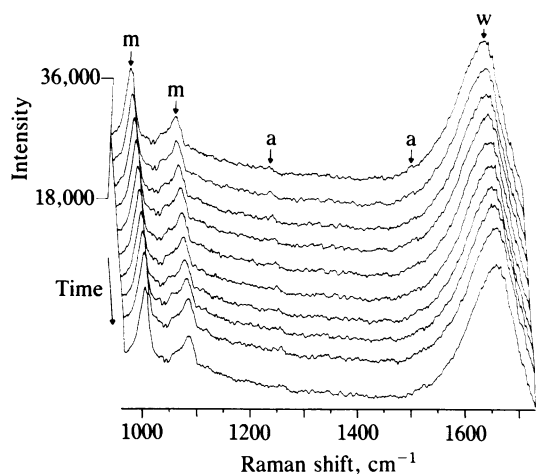


FIG. 2. Time-sequenced Raman spectra of minimal medium (10 tracks).

those at 1640 cm^{-1} to water. They are denoted by the letters "m" and "w" above the spectra. The weak but persistent structures in the baseline at 1250 and 1520 cm^{-1} are assigned to variations (1–2%) in the sensitivity of the OMA Reticon array. They are denoted by the letter "a" above the spectra. Smaller fluctuations in the baseline represent the level of noise in the spectra.

A typical time sequence of Raman spectra of asynchronous *E. coli*, where time is measured from the moment the asynchronous culture is placed in the holding vessel (Fig. 1) is shown in Fig. 3. At the first track (20 min), bacterial concentrations are 6.9×10^7 per ml and at the last (60 min) concentrations have reached 1.0×10^8 per ml. Total elapsed time for the 40 tracks was 40 min, with 30-sec integrations for each track and 30 sec between tracks. Examination of these spectra reveals the Raman bands assignable to minimal medium (m), to water (w), and to detector variations (a) but not to bacteria. There is a small temporal variation (3–4%) in the intensity of the baseline that reflects the degree of background noise fluctuation for the experiment. Such fluctuations are generated by variations in detector sensitivity, in laser power, and in bacterial flow or density. This relatively

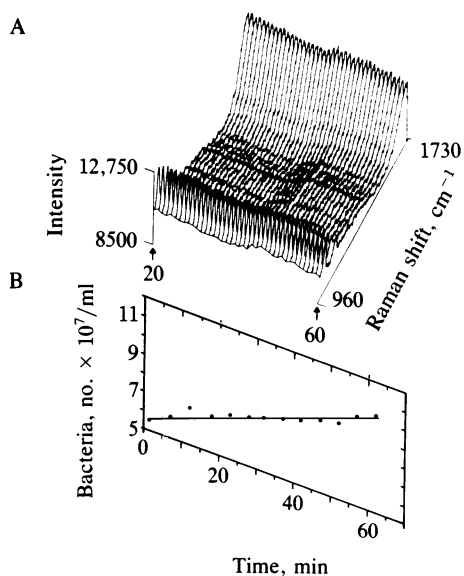


FIG. 3. (A) Time-sequenced Raman spectra of asynchronous *E. coli* (40 tracks). (B) The growth curve is a least-squares fit that indicates a cell doubling time of 70 min.

stable baseline serves as a control for subsequent time-sequenced spectra of synchronous cultures.

A time-sequenced Raman spectrum of synchronously dividing *E. coli* is shown in Fig. 4. Here time is measured from the moment the bacteria are collected from the synchronization apparatus. At the first track (35 min), bacterial concentrations are 3.1×10^7 per ml and, at the last (74 min), concentrations have reached 6.3×10^7 per ml. The "jump" in cell concentration (due to synchronized cell division) is the essential signature of synchronous cultures. Elapsed time for the 40 tracks is 40 min, with 30-sec integrations for each track and 30 sec between tracks. Particular attention should be focused on the unusual behavior of the entire baseline. When the cell division process is 90% completed at 57 min, the baseline begins to increase at a rate that cannot be assigned to experimental noise. This increase continues until 65 min, when it reaches a maximum that is 35% larger than its starting value. The maximum coincides with the emergence of newly formed daughter bacteria and occurs when the division cycle is completed. As the larger population of daughter bacteria start to grow, the baseline begins to decline (66–74 min). This unusual behavior has been observed for six out of seven synchronous cultures summarized in Table 1. It has not been observed for asynchronous cultures.

In a further effort to reveal small Raman features that might otherwise be obscured by noise, the data in Fig. 5 were cross-correlated with a lorentzian of variable width. In most cases, a lorentzian width (L) of 5 cm^{-1} was found to yield the best enhancement of known Raman features. This reduced the standard deviation (σ) of the noise by the factor $\{[(1/2) + (\pi/4)(L)]\}^{1/2}$. Aside from the minimal medium peaks (m), the water peak (w), and the artifacts due to the Reticon array (a), we see no structure that is significant at the 2σ level. In addition to this, we have examined cross-correlated data (using values of L from 3 to 10 cm^{-1}) for all the experiments summarized in Table 1. Aside from bands related to m, w, and a, there is no evidence for statistically significant peaks.

From Fig. 4, it is evident that the rising baseline has a broad peak centered near the middle of the spectral axis. This is examined in more detail in Fig. 6, which presents two individual spectra taken from Fig. 4. Spectrum A was recorded at 57 min, just before the baseline began its abrupt climb. Spectrum B was recorded at 65 min, when the baseline reached its maximum value. We can see that the minimal medium (m) and water (w) bands are relatively obscured in

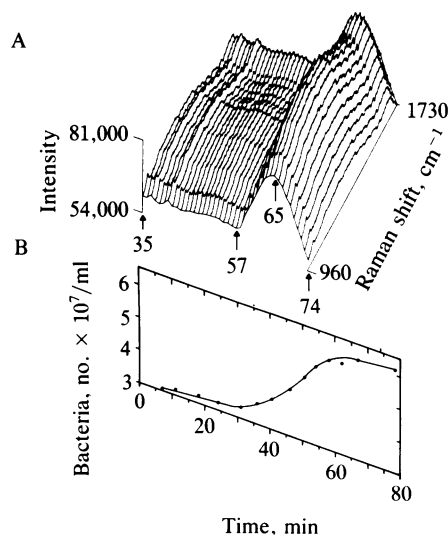


FIG. 4. (A) Time-sequenced Raman spectra of synchronous *E. coli* (40 tracks). (B) The growth curve indicates a cell doubling time of 48 min.

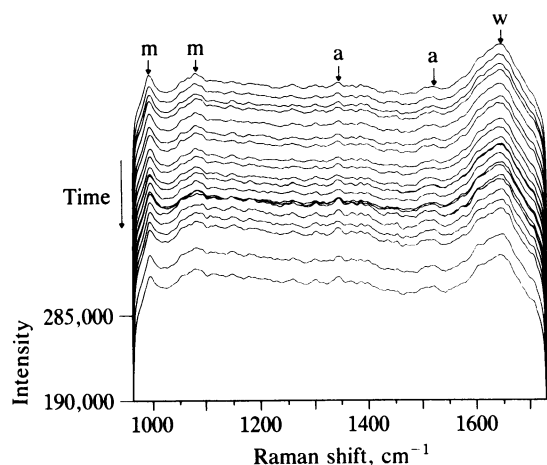


FIG. 5. Time-sequenced Raman spectra of synchronous *E. coli* (30 tracks). This spectra is from a different view angle than Fig. 4, as indicated by the arrow in that figure. It was cross-correlated with a L 5 cm^{-1} wide.

spectrum B, when compared with spectrum A, by the broad peak that centers on 1300 cm^{-1} . Spectrum C was generated by subtracting spectrum A from spectrum B. This manipulation reveals the broad fluorescent peak that is centered near 1300 cm^{-1} . This Raman shift corresponds to a wavelength around 550 nm , where flavin (isoalloxazine ring) cofactors are known to fluoresce strongly (33).

DISCUSSION

There are two plausible explanations for the time-dependent change in bacterial fluorescence. The first one involves a variation of the oxidation–reduction state of flavin cofactors. The second one involves a variation of the intracellular optical field.

Redox State. *E. coli* that are multiplying in a state of “balanced growth” are continually regulating their enzymatic machinery, to keep their supply of ATP and ADP invariant. This overall supply has often been referred to as the “energy charge” of bacteria (34). After a synchronous culture of bacteria divide, it is plausible (although not verified) that the newly emerged daughter cells temporarily require an increased supply of energy. One way to meet this energy demand rapidly, so that the energy charge of cells in the culture remains constant, is for the bacteria to adjust the redox state of their nucleotide cofactors. Such a temporary

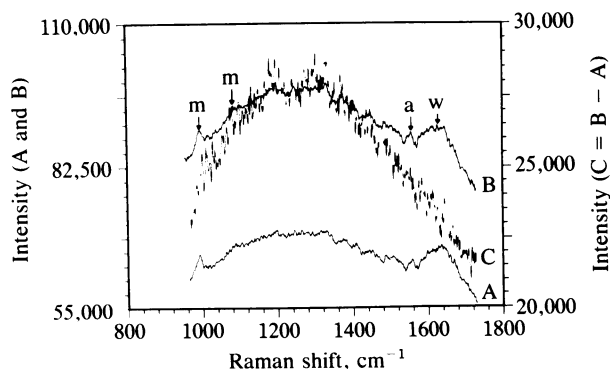


FIG. 6. Two spectra from Fig. 4 demonstrate the change in fluorescence after synchronous bacteria divide. Spectra A and B were recorded at 57 and 65 min, respectively. Subtracting spectrum A from spectrum B produces spectrum C, which reveals a broad fluorescent peak with a maximum at 1300 cm^{-1} (wavelength $\approx 550 \text{ nm}$).

adjustment would result in a decreased concentration of reduced “high-energy” cofactors and an increased concentration of oxidized “low-energy” cofactors.

FAD and FMN are essential cofactors in bacterial metabolism. Their oxidation–reduction states are closely tied to the redox states of the pyridine nucleotides NADH_2/NAD and $\text{NADPH}_2/\text{NADP}$ that act as regulators of metabolic pathways and as immediate reservoirs of bacterial energy. When these flavin cofactors are oxidized (FAD and FMN), they are among the most fluorescent compounds in bacteria but when they are reduced (FADH_2 and FMNH_2), they are not fluorescent. Therefore, it is tempting to speculate that the increase we have observed in bacterial fluorescence is due (in part) to the oxidation of flavin cofactors. This transient oxidation may reflect adjustable relationships between the energy regulatory mechanisms of newly emerged bacteria.

In addition, we have observed similar increases in bacterial fluorescence immediately after collecting cells from the effluent of the synchronization apparatus. This finding is consistent with the idea that cofactors in daughter cells are relatively “oxidized”. However, transient increases in oxygen concentration within bacteria (which could change the redox state of flavin cofactors) might also be attributed to (i) an increased surface to volume ratio of newly emerged daughter cells or (ii) an increased oxygen concentration in minimal media during the cell synchronization and collection process. These possibilities offer a second explanation for the increase in oxidized cofactors that have not been eliminated.

Internal Optical-Field Variations. When an optical field is incident upon a bacterium, the fact that the cell walls have a higher index of refraction than the medium or the intracellular substance (both of which are mainly water) results in a small fraction of the light being reflected (or scattered) while the rest is transmitted. The laser light that is transmitted through the bacterium can experience interference between the “entrance” wall on one side of the cell and the “exit” wall on the opposite side. This interference effect creates standing optical waves inside the bacteria and results in optical-field intensity variations that depend on intracellular position.

During the cell division process, substantial changes take place in the size of the average bacterium. These changes can appreciably alter the distribution of standing-wave optical-field intensities (from the laser illumination) at various locations within the cell. Since laser light absorption by bacterial components (such as flavin cofactors that are concentrated at the inner membrane) is proportional to the local optical intensity, consequent changes in bacterial fluorescence can occur. Further, since the diameter of a bacterium is approximately equal to the wavelength of the illuminating laser ($\lambda \approx 0.5 \mu\text{m}$) and the cell wall itself is considerably thinner ($\approx 0.1 \lambda$), these interferometric effects (as the bacterial size changes) can account for local intracellular intensity changes of up to 30%.

These effects cannot generally be calculated analytically (35) and usually require numerical methods that assume various idealized representations of the cell structure. We have performed numerical calculations, based on a one-dimensional idealization of the cell structure, that assume a simplified three-layer model for the Gram-negative cell wall. Although these results rely on rough estimates of cell wall thickness and index of refraction, they indicate that variations in the internal optical field may account for some of the observed changes in bacterial fluorescence.

Narrow Versus Broad Peaks. Previous studies of active bacteria by Webb (13, 36), have emphasized that division synchrony is essential to the investigation of metabolically induced Raman activity. These studies have also reported that the location of Raman “metabolic peaks” varies with the phase of the division cycle. The data presented here partially agree with this finding. However, our results indicate that

metabolic peaks are assignable to changes in bacterial fluorescence.

Raman "peaks" that have been ascribed to metabolic activity in previous reports can be characterized as either narrow ($5\text{--}30\text{ cm}^{-1}$) or broad ($100\text{--}300\text{ cm}^{-1}$). The origin of these two different widths of peaks can be assigned to separate mechanisms that have not previously been fully appreciated. The generation of narrow peaks has been discussed by O'Sullivan and Santo (27). For studies using scanning monochromators they point that (i) clumps of cells may elastically scatter light thereby generating baseline variations, because of incomplete rejection by the monochromator, at the frequency of the laser (causing false lines only in the low-frequency region) and (ii) clumps of cells passing through the laser beam may fluoresce causing false lines to appear that are further red shifted from the frequency of the laser. In both cases, various particle densities interact with the laser-beam to cause variations in the baseline. The "width" of these variations will depend on the scanning rate of the monochromator, on the resolution of the monochromator, and on the motion of the particle. In many spectra, we have seen substantial (5–10%) variations in baseline intensity that could have generated false peaks with a scanning monochromator. By comparing Fig. 2 to Fig. 3, it is apparent that the presence of bacteria increases baseline variability. This explanation may account for narrow "spikes" and peaks but it does not satisfactorily account for the generation of broader peaks reported in several papers (13, 20, 21).

The results presented here show how a scanning monochromator could generate the broader peaks associated with synchronous bacterial cultures. We have shown that division synchrony results in a time-dependent increase in bacterial fluorescence that is correlated with the cell fission cycle. Several examples of broad peaks are shown by Webb (13), where the monochromator scanning time (to record a peak) took 1–2 min and by Bannikov *et al.* (20), where the scanning time took 2–7 min.

Continuous oscillations in the redox state of pyridine nucleotides (with periods from 30 to 300 sec) have also been observed in synchronous cultures of *Klebsiella aerogenes* (a close relative of *E. coli*) and several other single cell organisms (37). These oscillations occur spontaneously throughout the entire growth cycle and are thought to be generated by phase differences between the regulatory enzymes of the glycolytic pathway (38). Although these changes in fluorescence are generated by a different mechanism than suggested above, glycolytic oscillations can account for highly periodic changes in bacterial fluorescence. Examples of such peaks are also shown in refs. 13 (pp. 213 and 215) and 20.

Considering the good agreement previously reported between Webb's Raman spectra observed in the range of $20\text{ to }200\text{ cm}^{-1}$ and numerical computations based on Davydov's soliton (14, 15), our failure to observe Raman bands that could be assigned to the metabolic process was disappointing.

CONCLUSIONS

1. At concentrations of $10^7\text{--}10^8$ cells per ml, *E. coli* cultures have not revealed Raman bands assignable to the metabolic process nor to the chemical composition of the bacteria.

2. For synchronous cultures, we have observed a transient increase in bacterial fluorescence that is correlated with the division cycle. For asynchronous cultures, this increase in fluorescence is not observed. We have not conclusively identified the mechanism of fluorescence variation but have suggested the possibility of redox or optical effects.

3. Time-dependent variations in bacterial fluorescence offer a plausible explanation for some of the previously reported laser-Raman spectra of synchronous cultures.

4. It is our view that future experiments in this area should incorporate an OMA detection system. Such instrumentation avoids artifacts associated with a variable baseline and increases the rate of data collection by a factor that is approximately half the number of active channels in the OMA.

It is a pleasure to thank Charles E. Helmstetter, Arthur L. Koch, and Sydney J. Webb for helpful discussions. We also thank Dennis Gill for the optical-field calculations. This work was performed under the auspices of the Department of Energy and was supported in part by a grant from the Naval Air Systems Command (MIPR N0001984MP-47836).

- Fröhlich, H. (1968) *Int. J. Quantum Chem.* **2**, 641–649.
- Fröhlich, H. (1983) in *Coherent Excitations in Biological Systems*, eds. Fröhlich, H. & Kremer, F. (Springer, Berlin), pp. 1–5.
- Davydov, A. S. (1973) *J. Theor. Biol.* **38**, 559–569.
- Davydov, A. S. (1982) *Biology and Quantum Mechanics* (Pergamon, Oxford), pp. 185–212.
- Bilz, H., Büttner, H. & Fröhlich, H. (1981) *Z. Naturforsch. B* **36**, 208–212.
- Cooper, M. S. (1981) *Collect. Phenom.* **3**, 273–288.
- Del Giudice, E., Doglia, S. & Milani, M. (1982) *Phys. Scr.* **26**, 232–238.
- Webb, S. J. & Dodds, D. D. (1968) *Nature (London)* **218**, 374–375.
- Webb, S. J. & Booth, A. D. (1969) *Nature (London)* **222**, 1199–1200.
- Devyatkov, N. D. (1973) *Usp. Fiz. Nauk.* **110**, 452–454 [(1974) *Sov. Phys. Usp.* (Engl. Trans.) **16**, 568–569].
- Berteaud, A. J., Dardalhon, M., Rebeyrotte, N. & Averbek, D. (1975) *C. R. Acad. Sci. Paris D* **281**, 843–846.
- Grundler, W. & Keilman, F. (1983) *Phys. Rev. Lett.* **51**, 1214–1216.
- Webb, S. J. (1980) *Phys. Rep.* **60**, 201–224.
- Scott, A. C. (1981) *Phys. Lett. A* **86**, 60–62.
- Lomdahl, P. S., MacNeil, L., Scott, A. C., Stoneham, M. E. & Webb, S. J. (1982) *Phys. Lett. A* **92**, 207–210.
- Cooper, M. S. & Amer, N. M. (1983) *Phys. Lett. A* **98**, 138–140.
- Furia, L. & Gandhi, Om P. (1984) *Phys. Lett. A* **102**, 380–382.
- Kinoshita, S., Kuniko, H. & Kushida, T. (1980) *J. Phys. Soc. Jpn.* **49**, 314–321.
- Drissler, F. & Macfarlane, R. M. (1978) *Phys. Lett. A* **69**, 65–67.
- Bannikov, V. S., Bezruchko, S. M., Grishankova, E. V., Kuz'min, S. B., Mityagin, Y. A., Orlov, R. Y., Rozhkov, S. B. & Sokolina, V. A. (1980) *Dokl. Akad. Nauk SSSR* **253**, 479–480 [(1980) *Dokl. Biophys.* (Engl. Trans.) **253**, 119–120].
- Drissler, F. & Santo, L. (1983) in *Coherent Excitations in Biological Systems*, eds. Fröhlich, H. & Kremer, F. (Springer, Berlin), pp. 6–9.
- Hyman, J. M., McLaughlin, D. W. & Scott, A. C. (1981) *Physica 3D* **1** & **2**, 23–44.
- Scott, A. C. (1982) *Phys. Rev. A* **26**, 578–595.
- Scott, A. C. (1983) *Phys. Rev. A* **27**, 2767.
- Scott, A. C. (1982) *Phys. Scr.* **25**, 651–658.
- Lomdahl, P. S., Layne, S. P. & Bigio, I. J. (1984) *Los Alamos Sci.* **10**, 2–22.
- O'Sullivan, R. A. & Santo, L. (1981) *Can. J. Spectrosc.* **26**, 143–148.
- Helmstetter, C. E. (1969) in *Methods in Microbiology*, eds. Norris, J. R. & Ribbons, D. W. (Academic, London), Vol. 1, pp. 327–363.
- Lloyd, D., Poole, R. K. & Edwards, S. W. (1982) *The Cell Division Cycle* (Academic, London), p. 45.
- Helmstetter, C. E. (1974) *J. Mol. Biol.* **84**, 1–19.
- Kubitschek, H. E. (1969) in *Methods in Microbiology*, eds. Norris, J. R. & Ribbons, D. W. (Academic, London), Vol. 1, pp. 593–610.
- Koch, A. L. (1981) in *Manual of Methods for General Bacteriology*, ed. Gerhardt, P. (Am Soc Microbiol), pp. 179–207.
- Nishimura, Y. & Tsuboi, M. (1978) *Chem. Phys. Lett.* **59**, 210–213.
- Ingraham, J. L., Maaløe, O. & Niedhardt, F. C. (1983) *Growth of the Bacterial Cell* (Sinauer, Sunderland, MA), pp. 163–168.
- Kerker, M. (1969) *The Scattering of Light and Other Electromagnetic Radiation* (Academic, New York).
- Webb, S. J. (1981) *Collect. Phenom.* **3**, 313–320.
- Harrison, D. E. F. (1970) *J. Cell Biol.* **45**, 514–521.
- Winfree, A. T. (1980) *The Geometry of Biological Time* (Springer, New York), pp. 285–299.